

# Metallic artifact reduction by evaluation of the additional value of iterative reconstruction algorithms in hip prosthesis computed tomography imaging

Angeliki Neroladaki, MD, Steve Philippe Martin, MD, Ilias Bagetakos, MD, Diomidis Botsikas, MD, Marion Hamard, MD, Xavier Montet, MD, Sana Boudabbous, MD\*

## Abstract

To evaluate iterative metal artifact reduction (iMAR) technique in images data of hip prosthesis on computed tomography (CT) and the added value of advanced modeled iterative reconstruction (ADMIRE) compared with standard filtered back projection (FBP).

Twenty-eight patients addressed to CT examinations for hip prosthesis were included prospectively. Images were reconstructed with iMAR algorithm in addition to FBP and ADMIRE techniques. Measuring image noise assessed objective image quality and attenuation values with standardized region of interest (ROI) in 4 predefined anatomical structures (gluteus medius and rectus femoris muscles, inferior and anterior abdominal fat, and femoral vessels when contrast media was present). Subjective image quality was graded on a 5-point Likert scale, taking into account the size of artifacts, the metal–bone interface and the conspicuity of pelvic organs, and the diagnostic confidence.

Improvement in overall image quality was statistically significant using iMAR ( $P < .001$ ) compared with ADMIRE and FBP. ADMIRE did not show any impact in image noise, attenuation value, or global quality image. iMAR showed a significant decrease in image noise in all ROIs (Hounsfield Unit) as compared with FBP and ADMIRE. Interobserver agreement was high in all reconstructions (FBP, FBP+iMAR, ADMIRE, and ADMIRE + iMAR) more than 0.8. iMAR reconstructions showed emergence of new artifacts in bone–metal interface.

iMAR algorithm allows a significant reduction of metal artifacts on CT images with unilateral or bilateral prostheses without additional value of ADMIRE. It improves the analysis of surrounding tissue but potentially generates new artifacts in bone–metal interface.

**Abbreviations:** ADMIRE = advanced modeled iterative reconstruction, ANOVA = ordinary one-way analysis of variation, BMI = body mass index, CT = computed tomography, DECT = dual-energy computed tomography, FBP = filtered back projection, HU = Hounsfield Unit, iMAR = iterative metal artifact reduction, IR = iterative reconstruction, LI = linear interpolation, MAR = metal artifact reduction, MDT = metal deletion technique, MRI = magnetic resonance imaging, RMAR = refinement metallic artifact reduction, ROI = region of interest, SD = standard deviation, SPECT-CT = single-photon emission CT.

**Keywords:** algorithms, artifacts, hip prosthesis

## 1. Introduction

Metal artifacts from large implants like hip prostheses are a common problem in computed tomography (CT) imaging. Artifacts are caused by beam hardening and photon starvation.<sup>[1]</sup>

Editor: Hyunjin Park.

This research did not receive any specific grant from funding agencies in the public, commercial, or not-for-profit sectors.

The authors have no conflicts of interest to disclose.

Radiology Department, Geneva University Hospital, Genève, Switzerland.

\* Correspondence: Sana Boudabbous, Radiology Department, Geneva University Hospital, Rue Gabrielle-Perret-Gentil 4, 1211 Genève 4, Switzerland (e-mail: Sana.boudabbous@hcuge.ch).

Copyright © 2019 the Author(s). Published by Wolters Kluwer Health, Inc. This is an open access article distributed under the terms of the Creative Commons Attribution-Non Commercial-No Derivatives License 4.0 (CCBY-NC-ND), where it is permissible to download and share the work provided it is properly cited. The work cannot be changed in any way or used commercially without permission from the journal.

Medicine (2019) 98:6(e14341)

Received: 16 August 2018 / Received in final form: 2 January 2019 / Accepted: 4 January 2019

<http://dx.doi.org/10.1097/MD.0000000000014341>

Methods for reducing artifacts used in routine practice, such as increasing tube current, cause higher radiation doses to the patient yet limited improvement of image quality. Several methods have been developed to reduce artifacts in surrounding tissues and bone–metal interface. Metal artifact reduction (MAR) algorithms have been proposed and widely studied in the literature.<sup>[2–6]</sup> These algorithms worked on raw projection data like iterative reconstruction (IR) methods and were evaluated for small and large implants.<sup>[7–9]</sup> The results showed improved image quality and diagnostic accuracy. Several studies demonstrated that MAR improves diagnostic assessment in the surrounding tissues and the bone–implant interface.<sup>[10]</sup> In routine clinical practice, IR algorithms are available and used mainly for x-ray dose reduction, enabling significant dose reduction while maintaining image quality.<sup>[11–13]</sup> These algorithms detect noise-related artifacts and compare them in the projection and image domains, serving as a potential method to reduce metallic artifacts.<sup>[14]</sup> The purpose of this study was to quantitatively and qualitatively evaluate the impact of a new iMAR algorithm on overall image quality and diagnosis compared with filtered back projection (FBP) in hip prosthesis in clinical routine practice, with special focus on bone–metal interface regarding new artifacts produced by this algorithm.<sup>[15]</sup> We also evaluated the impact of

advanced modeled iterative reconstruction (ADMIRE); the third and latest generation of IR from Siemens in artifact reduction. In addition, we evaluated the accuracy and agreement between readers to detect pathologies localized near metal as well as in the surrounding soft tissue.

## 2. Materials and methods

### 2.1. Patient population

The local Swiss ethics committee on research involving humans approved this prospective study and waived the need for written patient consent. Patient data was anonymized. Patients referred to the department for pelvic CT examination for hip prostheses complication (loosening, septic complication, prosthesis dislocation, periprosthetic fracture) were included consecutively.

Between March and October 2016, a total of 28 patients (men: 14; women: 14; mean age: 75.14 years) were included consecutively in the analysis; 21 patients had a unilateral hip prosthesis and 7 a bilateral hip prosthesis. The mean of body mass index (BMI) was 22.47.

### 2.2. Computed tomography protocol and image reconstruction

All CT scans were performed using a second-generation dual-energy computed tomography (DECT) scanner (SOMATOM Definition Flash, Siemens Healthcare, Forchheim, Germany). A standard single-energy protocol (120 kV) was applied in all patients. Pitch was always set from 0.45 to 0.9, and collimation was  $64 \times 0.6$  mm. When contrast medium was clinically indicated (80–120 mL of Accupaque 350, GE Healthcare, Opfikon, Switzerland) were injected at a flow rate of 3 mL/s and flushed out by 40 mL of saline solution at a flow rate of 3 mL/s. Five cases of injected CT were carried out to exclude collection in prostheses surrounding tissues. All CT scans were performed in single energy acquisition (X ray tube current: 300 mAs) with utilization of automatic exposure control (Care dose, Siemens; Forchheim, Germany). The raw datasets were then reconstructed with FBP and ADMIRE level 3 with and without iMAR (the level used in our department with reference to literature).<sup>[13]</sup> Hip prosthesis-dedicated iMAR was always chosen (the system proposes different iMAR algorithms, each dedicated to a specific

clinical question). We used a soft tissue kernel (B/I41f medium). The slice thickness interval was 1.5 mm. Four different reconstructed series were thus obtained for every patient: FBP, FBP+iMAR, ADMIRE, and ADMIRE+iMAR.

### 2.3. Qualitative image analysis

Subjective image analysis was performed in a double-blind mode with appropriate time interval (1 month) for all reconstructed series by 2 board-certified musculoskeletal radiologists with 3 and 1 years of experience, respectively. All reconstructions were displayed in a bone window (level 300/width 1500). The readers were allowed to optimize the images by adjusting the window parameters and analyzed 3 parameters: overall image quality, diagnostic confidence for the assessment of pelvic organs, and metal–bone interface. The Likert scores used are summarized in Table 1.<sup>[8]</sup>

Furthermore, all suspected cases of loosening in FBP + iMAR reconstructions were compared with standard pelvic x-rays, which are considered the gold standard<sup>[16]</sup> and diagnostic accuracy was calculated.

### 2.4. Quantitative image analysis

Image noise of FBP, FBP+iMAR, ADMIRE, and ADMIRE+iMAR was determined in an axial CT slice in predefined structures (region of interest [ROI] 1: gluteus medius muscle; ROI2: rectus femoris muscle; ROI3: subcutaneous fat; ROI4: femoral vessels in injected CT) by measuring standard deviation (SD) in a standardized circular ROI at the exact same location for every reconstruction.<sup>[7]</sup> The SD of the CT numbers was calculated in all 4 reconstructed images for every patient. To ensure reproducibility of measurements in the 4 different reconstructed series from the same single acquisition, standardized circular ROIs of 10 mm<sup>2</sup> were positioned in copy-paste mode and repeated for every series 2 times to allow data consistency.

### 2.5. Statistical analysis

All statistical analyses were performed using GraphPad Prism 6.0e (Macintosh Version by Software MacKiev 1994–2014 GraphPad Software, Inc, San Diego, California). Interobserver agreement of subjective image analysis was determined using

**Table 1**

**Likert scores of qualitative parameters analyzed: overall image quality, diagnostic confidence for the assessment of pelvic organs and metal–bone interface.**

|   |   |   |
|---|---|---|
| Image quality   | 1 | Massive streak artifacts and markedly reduced image quality   |
|   | 2 | Significant artifacts and limited image quality   |
|   | 3 | Minor artifacts and acceptable image quality  |
|   | 4 | Minor artifacts and good image quality  |
|   | 5 | Absence of artifacts and excellent image quality  |
| Diagnostic confidence for the assessment of pelvic organs | 1 | Marked artifacts, with nondiagnostic for most pelvic organs and hindering diagnostic decision-making  |
|   | 2 | Major artifacts without depicting most pelvic organs interfering with diagnostic decision-making      |
|   | 3 | Moderate artifacts for most pelvic organs but acceptable diagnostic quality                           |
|   | 4 | Minor artifacts, with good analysis the pelvic organs not interfering with diagnostic decision-making |
|   | 5 | No artifacts, with excellent analysis of pelvic organs enabling full diagnosis                        |
| Bone–cement–metal interface                               | 1 | Major artifacts hindering diagnostic decision-making  |
|   | 2 | Artifacts interfering with diagnostic decision-making   |
|   | 3 | Moderate artifacts but acceptable diagnostic decision-making  |
|   | 4 | Minor artifacts not interfering with diagnostic decision-making                                       |
|   | 5 | Complete absence of imaging artifacts   |

**Table 2****Comparison of median values of image quality, diagnostic confidence for the assessment of pelvic organs, and bone–metal interface.**

| Median (25–75 percentile) | Image quality | <i>P</i> values | Diagnostic confidence for the assessment of pelvic organs | <i>P</i> values | Bone–metal interface | <i>P</i> values |
|---------------------------|---------------|-----------------|---|-----------------|----------------------|-----------------|
| FBP                       | 1 (1–2)       | .2              | 2 (0.25–3)  | >.9999          | 1 (1–2)              | >.9999          |
| ADMIRE                    | 2 (1–2.75)    | <.0001          | 3 (0.25–3)  | <.0001          | 2 (1–2)              | <.0001          |
| FBP+ iMAR                 | 4 (3–4)       | >.9999          | 4 (4–4.75)  | >.9999          | 3 (2–3)              | >.9999          |
| ADMIRE + iMAR             | 3.5 (3–4)     |                 | 4 (4–4.75)  |                 | 3 (2–3)              |                 |

FBP = filtered back projection, ADMIRE = advanced model-based iterative reconstruction, iMAR = iterative metal artifact reduction.

Kendall *W* coefficient of concordance. Values of 0 to 0.2, 0.21 to 0.40, 0.41 to 0.60, 0.61 to 0.80, and 0.81 to 1.00 were considered to represent slight, fair, moderate, substantial, and almost perfect agreement, respectively. Normality of the data for subjective analysis was tested using the D'Agostino–Pearson omnibus normality test, the Shapiro–Wilk test, and the Kolmogorov–Smirnov normality test. Due to non-normally distributed values, comparison of the subjective analysis medians from FBP, ADMIRE, FBP+iMAR, and ADMIRE+iMAR was performed using the Friedman test. Results are given as medians and interquartile ranges. A *P* value of less than .05 was considered statistically significant. Quantitative data was compared using ordinary one-way analysis of variation (ANOVA) test given the normally-distributed values, with results presented as means and SDs also and statistical significance set at under 0.05.

### 3. Results

Twenty-eight patients and 35 prostheses (21 patients with unilateral and 7 with bilateral prostheses) were included in this study. Seven cases with bone–metal loosening, 5 cases with collection or gluteal bursal collection, and 3 cases with femoral

fracture around the stem were diagnosed. In the other cases, the CT was negative.

#### 3.1. Qualitative image analysis

The results of the subjective analysis are summarized in Table 2. All the studied parameters improved with the use of iMAR with *P* values <.001 for image quality, diagnostic confidence for the assessment of pelvic organs, and bone–metal interface whereas ADMIRE had no significant impact with *P* values >.09 respectively (Figs. 1 and 2). Interobserver agreement ranged from high to excellent for all parameters ( $W \geq 0.772$ ) (Table 3).

Concerning the comparison with the gold standard for loosening evaluation, we suspected bone loosening in 5 patients based on iMAR reconstruction yet were unable to confirm either with the FBP reconstruction or conventional radiography. These results were considered false positives (Fig. 3). We suspected bone loosening in 7 patients based on all CT reconstructions, which was also confirmed by conventional radiography (true positive). In all other cases, no loosening was detected, either using CT, FBP or iMAR reconstructions, nor in x-ray (true negative cases,

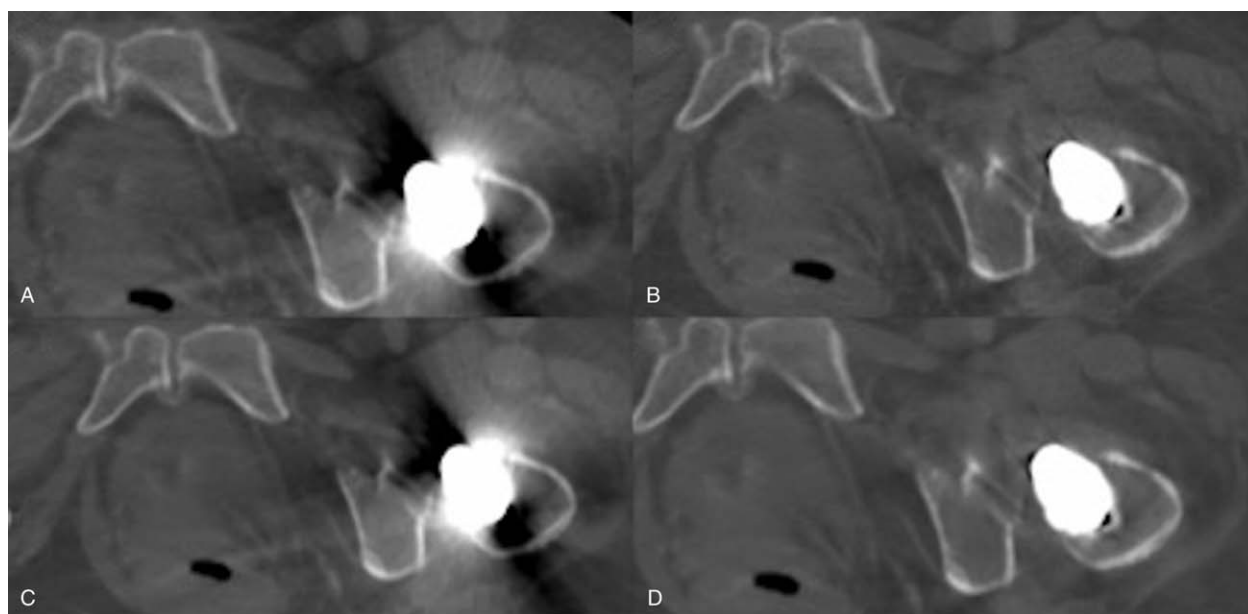


**Figure 1.** Artifact reduction in left hip arthroplasty in bone–metal interface and surrounding tissues when using iMAR (B, D) comparing with FBP (A) without impact of ADMIRE (C). iMAR = iterative metal artifact reduction, FBP = filtered back projection, ADMIRE = advanced modeled iterative reconstruction.

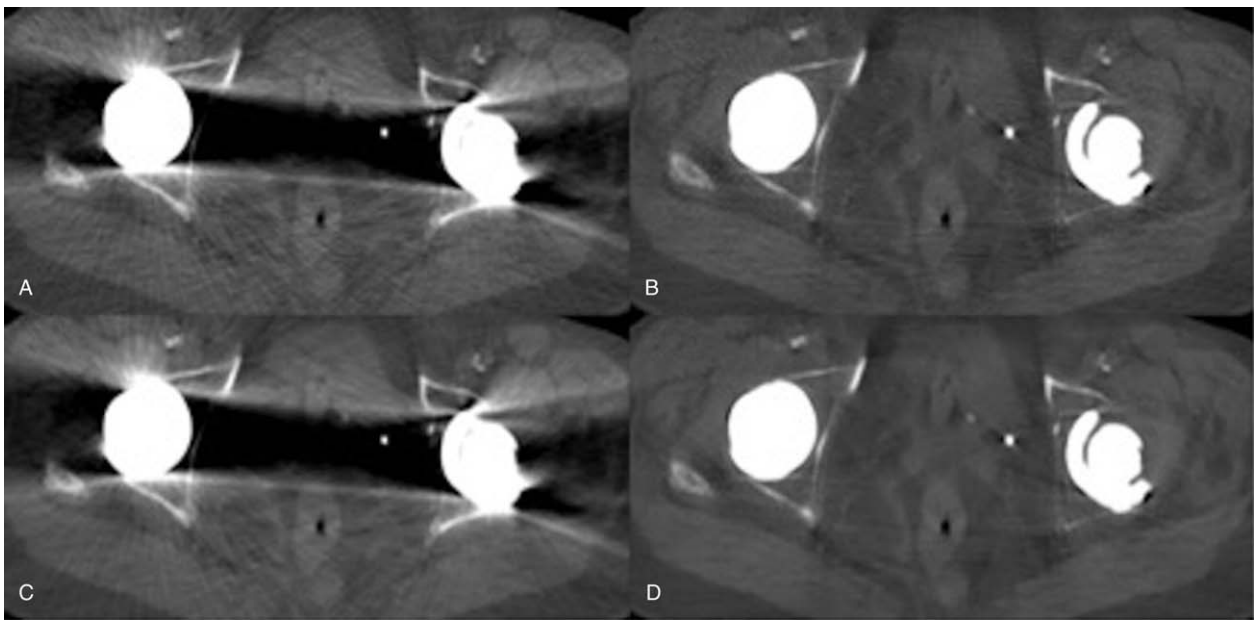


**Figure 2.** Case of bilateral hip prosthesis showing the improvement of image quality for pelvic organs in images constructed with iMAR (B, D), again without additional value of ADMIRE (C) compared with FBP (A). iMAR=iterative metal artifact reduction, FBP=filtered back projection, ADMIRE=advanced modeled iterative reconstruction.

**Table 3**

**Interobserver agreement of subjective image analysis using Kendall W coefficient of concordance.**

|  | <b>Kendall W coefficient of concordance (95% confidence intervals)</b> |
|--|--|
| Image quality                          | W=0.872  |
| diagnosis confidence for pelvic organs | W=0.890  |
| Metal–bone interface                   | W=0.796  |

n = 21). Thus, the accuracy of iMAR algorithm was 0.81 to detect metal–bone interface loosening.

**3.2. Quantitative image analysis**

The results of the objective image analysis are summarized in Table 4. When iMAR was not used, the density measured in the muscle was different from the standard values, with a very high SD and P values = .92 for gluteus medius and = .48 for rectus femoris, meaning that the measurements took into account streak artifacts. When iMAR was applied to the data, the measured



**Figure 3.** Pseudo-loosening. X-rays of right hip prosthesis showing no sign of loosening in bone-metal interface, especially in Gruen zone 7. Coronal CT reconstructions in FBP (b) showing a beam hardening artifact at this level hiding that area (or hindering the analysis) (thin white arrow); disappearance of this artifact in iMAR reconstruction (c) but creation of pseudo-loosening artifact (thick white arrow).



**Table 4**

**Comparison of computed tomography number values in muscles (Gluteus Medius and Rectus Femoris) and in intra-abdominal fat between FBP, ADMIRE, iMAR, and ADMIRE+iMAR.**

| Mean ( $\pm$ SD) | Gluteus medius   | P values | Rectus femoris  | P values | Intra-abdominal fat | P values |
|------------------|------------------|----------|-----------------|----------|---------------------|----------|
| FBP              | -25 ( $\pm$ 114) | .92      | 135 ( $\pm$ 66) | .61      | -85 ( $\pm$ 34)     | .48      |
| ADMIRE           | -23 ( $\pm$ 112) | .04      | 135 ( $\pm$ 66) | .0002    | -85 ( $\pm$ 32)     | .99      |
| FBP+ iMAR        | 31 ( $\pm$ 19)   | .63      | 55 ( $\pm$ 29)  | .73      | -83 ( $\pm$ 54)     | .99      |
| ADMIRE + iMAR    | 29 ( $\pm$ 19)   |          | 55 ( $\pm$ 29)  |          | -83 ( $\pm$ 21)     |          |

ADMIRE = advanced model-based iterative reconstruction, FBP = filtered back projection, iMAR = iterative metal artifact reduction, SD = standard deviation.

density corresponded to the expected values of muscle density and the SD was lower, meaning that streak artifacts almost disappeared with  $P$  values = .04 for gluteus medius and  $<.002$  for rectus femoris.

When the ROI was placed in the intra-abdominal fat, far from the metallic artifacts, the density measured always corresponded to fat density, with no advantages afforded with either iterative reconstruction algorithms (Table 4) and  $P$  values = .48, .99, and .99 respectively in FBP, ADMIRE, and FBP+ iMAR reconstructions.

#### 4. Discussion

In our study, we highlighted that iMAR reconstruction significantly reduced artifacts near metal and in the surrounding tissues, while also enabling accurate diagnosis for hip pain. iMAR had an impact on high- and low-density streak artifacts in surrounding tissues. However, we noted new artifacts mimicking prosthesis loosening, particularly in the proximal femur, as shown in our results.

Metal artifacts still present a challenge in hip prosthesis today. These artifacts are due to beam hardening and photon starvation.<sup>[17]</sup> This affects adjacent tissues, mainly in the pelvis. Increasing tube currents and using high kV energy improves image quality but also increases radiation doses.<sup>[18]</sup> The best-known reconstruction algorithm used in CT imaging, known as FBP, fails to reconstruct the image due to inaccurate projection data.<sup>[19]</sup> Dual energy makes it possible to reduce artifacts by using different absorption spectra.<sup>[20,21]</sup> Iterative methods<sup>[7,8]</sup> and sinogram inpainting technique including MAR algorithms which target the beam hardening artifacts<sup>[22]</sup> are increasingly used. Despite the fact that these approaches are available, the creation of new artifacts by new methods is a significant drawback, limiting their clinical use. Moreover, iterative and interpolated reconstructions that have been developed are limited by the need for additional postprocessing and dedicated workstations.<sup>[5]</sup> The sinogram inpainting techniques recently developed, offer visible benefits in reducing metal artifacts<sup>[2]</sup> and especially useful in hip arthroplasty as demonstrated in our study. These studies assessed subjective image quality and pelvic structures and reported significant reduction of artifacts and improvement of overall quality as in other types of metal implants (dental, spinal hardware, and fracture devices). These different techniques and studies, however, also demonstrated the appearance of new artifacts (high- and low-density streak) generated by different algorithms.

Many studies have recently undertaken to explain new artifact emergence.<sup>[23–26]</sup> The interpolated sinogram inpainting MAR

algorithm is a technique that interpolates the projection data using neighboring information with the aim of replacing the corrupted images. This algorithm causes secondary artifacts as the transition is not sufficiently smooth.<sup>[27]</sup> The second main method is the normalized metal artifact reduction that may originate from the same problem as linear interpolation (LI) and also increases secondary artifacts, particularly when the target contains more than 1 metal.<sup>[28]</sup> Recently, Peng et al<sup>[29]</sup> proposed another innovation, a Gaussian diffusion sinogram inpainting in a fan-beam scanner. iMAR is developed from sinogram inpainting, combining it with linear interpolation. FBP is used and then a metal image is created. This metal data is then replaced with interpolated data from adjacent projections.<sup>[30]</sup> This approach has 2 major limitations: the sharp transition between interpolated and noninterpolated data results in new streak artifacts, and the lost coverage around the metal cannot be recovered by interpolation, resulting in blurring. To resolve this problem, iMAR normalizes the sinogram before interpolation. The output image is used several times as the input image for the next iteration. High-frequency data is replaced with high-frequency data from the original FBP reconstruction to recapture the data near the metal edge.

To overcome this drawback of new artifacts, Treece<sup>[31]</sup> compared several algorithms on various phantom data sets and clinical data sets of hip CT scan and showed that metal deletion technique (MDT) and new algorithm (refinement metal artifact reduction [RMAR]) are able to reduce as well as other techniques metallic artifacts with better performance and less new artifacts on the far field.

Our study focused on a new commercial algorithm affording significant artifact reduction, as demonstrated recently by other studies in hip arthroplasty cases clinically suspected of potential material complications.<sup>[32]</sup> The results of this study demonstrated the emergence of new artifacts and pseudo-lucent areas in bone at the interface with the prosthesis mimicking loosening. This finding has a significant impact on CT interpretation considering one of the principal challenges of CT is to detect loosening. Until now, conventional radiography of hip and pelvis has been the gold standard for surgeons.<sup>[16]</sup> Despite the studies on CT, magnetic resonance imaging (MRI),<sup>[16]</sup> and single-photon emission CT (SPECT)-CT,<sup>[33]</sup> x-ray remains the gold standard for loosening detection. CT is more efficient in detecting collection in surrounding soft tissues, and when combined with artifact reduction protocols it is also efficient for joint effusion and analyzing bone– or cement–metal interface.

The new artifacts created by these algorithms that mimic loosening limit their use, and care should be taken when loosening is suspected.

Our findings thus confirm those of former studies. We compared ROI near arthroplasty and in distant tissues at cup and stem levels between FBP and iMAR. In objective results, attenuation values fluctuate in the muscles, attesting to the new artifacts created by iMAR.

In another hand, the ADMIRE technique is an iterative method and an available option to reduce radiation doses and optimize image quality mainly in cardiac imaging.<sup>[13,34–36]</sup> Its capacity to reduce metal artifacts is, however, nonsignificant with inconsistent clinical impact, as demonstrated in our study.

This study has some limitations. First, we included only a small number of patients, even though hip arthroplasty is widespread, because of our including patients undergoing pelvis CT only to exclude arthroplasty complications. The readers were blinded to CT analysis for subjective findings, but the remarkable difference between FBP and iMAR could influence the subjective analysis, even when the images were interpreted several weeks apart. iMAR is a commercial technique available from 1 constructor. This study evaluated the impact of additional iterative reconstruction (ADMIRE) but did not evaluate the advantages of iMAR when scanning at lower energies. Our study confirmed the superiority of iMAR over FBP in terms of image quality and artifact reduction yet provided contrary findings to those of Subhas et al<sup>[31]</sup> in terms of its ability to detect pathologic lesions near prosthesis with more confidence in a phantom model. It should not be forgotten that reconstructions are performed instantly, and with the increasing availability of these techniques from multiple constructors this technique could be used in routine practice. Comparison with FBP is mandatory, and it is even recommended to compare with other techniques (x-ray, MRI, or SPECT-CT) to avoid false-positive diagnosis of bone loosening on iMAR images, which is still a concern with sinogram inpainting techniques.

## 5. Conclusion

This work confirms the commercially-available technique iMAR's capacity to improve image quality as well as to reduce metal artifacts due to hip prosthesis. The combination of further iterative reconstruction (developed for dose reduction) has not proven to be of additional value for decreasing metal artifacts. The emergence of new artifacts in the bone-metal interface means vigilant analysis of iMAR reconstructions is required, as well as simultaneous reading with standard reconstructions in addition to comparison with other imaging modalities.

## Author contributions

**Conceptualization:** Angeliki Neroladaki, Ilias Bagetakos, Diomidis Botsikas.

**Data curation:** Angeliki Neroladaki, Steve Philippe Martin, Sana Boudabbous.

**Formal analysis:** Ilias Bagetakos, Marion Hamard, Sana Boudabbous.

**Investigation:** Angeliki Neroladaki, Diomidis Botsikas, Sana Boudabbous.

**Methodology:** Steve Philippe Martin, Xavier Montet, Sana Boudabbous.

**Resources:** Angeliki Neroladaki, Diomidis Botsikas.

**Software:** Steve Philippe Martin, Ilias Bagetakos, Marion Hamard.

**Supervision:** Sana Boudabbous.

**Validation:** Steve Philippe Martin, Xavier Montet, Sana Boudabbous.

**Visualization:** Marion Hamard, Sana Boudabbous.

**Writing – original draft:** Sana Boudabbous.

**Writing – review & editing:** Xavier Montet, Sana Boudabbous.

## References

- [1] Pessis E, Campagna R, Sverzut JM, et al. Virtual monochromatic spectral imaging with fast kilovoltage switching: reduction of metal artifacts at CT. *Radiographics* 2013;33:573–83.
- [2] Andersson KM, Nowik P, Persliden J, et al. Metal artifact reduction in CT imaging of hip prostheses—an evaluation of commercial techniques provided by four vendors. *Br J Radiol* 2015;88:20140473.
- [3] Boomsma MF, Warringa N, Edens MA, et al. Quantitative analysis of orthopedic metal artifact reduction in 64-slice computed tomography scans in large head metal-on-metal total hip replacement, a phantom study. *Springerplus* 2016;5:405.
- [4] Abdoli M, Mehranian A, Ailianou A, et al. Assessment of metal artifact reduction methods in pelvic CT. *Med Phys* 2016;43:1588–97.
- [5] Jeong S, Kim SH, Hwang EJ, et al. Usefulness of a metal artifact reduction algorithm for orthopedic implants in abdominal CT: phantom and clinical study results. *AJR Am J Roentgenol* 2015;204:307–17.
- [6] Liu PT, Pavlicek WP, Peter MB, et al. Metal artifact reduction image reconstruction algorithm for CT of implanted metal orthopedic devices: a work in progress. *Skeletal Radiol* 2009;38:797–802.
- [7] Morsbach F, Bickelhaupt S, Wanner GA, et al. Reduction of metal artifacts from hip prostheses on CT images of the pelvis: value of iterative reconstructions. *Radiology* 2013;68:237–44.
- [8] Morsbach F, Wurnig M, Kunz DM, et al. Metal artifact reduction from dental hardware in carotid CT angiography using iterative reconstructions. *Eur Radiol* 2013;23:2687–94.
- [9] Sonoda A, Nitta N, Ushio N, et al. Evaluation of the quality of CT images acquired with the single energy metal artifact reduction (SEMAR) algorithm in patients with hip and dental prostheses and aneurysm embolization coils. *Jpn J Radiol* 2015;33:710–6.
- [10] Bongers MN, Schabel C, Thomas C, et al. Comparison and combination of dual-energy- and iterative-based metal artifact reduction on hip prosthesis and dental implants. *PLoS One* 2015;10:e0143584.
- [11] Neroladaki A, Botsikas D, Boudabbous S, et al. Computed tomography of the chest with model-based iterative reconstruction using a radiation exposure similar to chest X-ray examination: preliminary observations. *Eur Radiol* 2013;23:360–6.
- [12] Botsikas D, Stefanelli S, Boudabbous S, et al. Model-based iterative reconstruction versus adaptive statistical iterative reconstruction in low-dose abdominal CT for urolithiasis. *AJR Am J Roentgenol* 2014;203:336–40.
- [13] Schaller F, Sedlmair M, Raupach R, et al. Noise reduction in abdominal computed tomography applying iterative reconstruction (ADMIRE). *Acad Radiol* 2016;23:1230–8.
- [14] Boudabbous S, Arditi D, Paulin E, et al. Model-based iterative reconstruction (MBIR) for the reduction of metal artifacts on CT. *AJR Am J Roentgenol* 2015;205:380–5.
- [15] Fitsiori A, Martin SP, Juillet De Saint Lager A, et al. Iterative algorithms applied to treated intracranial aneurysms. *Clin Neuroradiol*. 2018 [Epub ahead of print].
- [16] Fritz J, Lurie B, Miller TT. Imaging of hip arthroplasty. *Semin Musculoskelet Radiol* 2013;17:316–27.
- [17] Weiß J, Schabel C, Bongers M, et al. Impact of iterative metal artifact reduction on diagnostic image quality in patients with dental hardware. *Acta Radiol* 2017;58:279–85.
- [18] Lee MJ, Kim S, Lee SA, et al. Overcoming artifacts from metallic orthopedic implants at high-field-strength MR imaging and multi-detector CT. *Radiographics*. 2007;27:791–803.
- [19] Wang T, Nakamoto K, Zhang H, et al. Reweighted anisotropic total variation minimization for limited-angle CT reconstruction. *IEEE Trans Nucl Sci* 2017;64:2742–2760.
- [20] Bamberg F, Dierks A, Nikolaou K, et al. Metal artifact reduction by dual energy computed tomography using monoenergetic extrapolation. *Eur Radiol* 2011;21:1424–9.
- [21] Meinel FG, Bischoff B, Zhang Q, et al. Metal artifact reduction by dual-energy computed tomography using energetic extrapolation: a systematically optimized protocol. *Invest Radiol* 2012;47:406–14.
- [22] Abdoli M, Ay MR, Ahmadian A, et al. Reduction of dental filling metallic artifacts in CT-based attenuation correction of PET data using weighted virtual optimized by a genetic algorithm. *Med Phys* 2010;37:6166–77.

- [23] Müller J, Buzug TM. Spurious structures created by interpolation-based CT metal artifact reduction. *Proc. SPIE* 2009;7258 1:1Y1–1Y8.
- [24] Mahnken AH, Raupach R, Wildberger JE, et al. A new algorithm for metal artifact reduction in computed tomography: in vitro and in vivo evaluation after total hip replacement. *Invest Radiol* 2003;38:769–75.
- [25] Oehler M, Buzug TM. Statistical image reconstruction for inconsistent CT projection data. *Methods Inf Med* 2007;3:261–9.
- [26] Veldkamp WJ, Joemai RM, van der Molen AJ, et al. Development and validation of segmentation and interpolation techniques in sinograms for metal artifact suppression in CT. *Med Phys* 2010;37:620–8.
- [27] Kalender WA, Hebel R, Ebersberger J. Reduction of CT artifacts caused by metallic implants. *Radiology* 1987;164:576–7.
- [28] Meyer E, Raupach R, Lell M, et al. Normalized metal artifact reduction (NMAR) in computed tomography. *Med Phys* 2010;37:5482–93.
- [29] Peng C, Qiu B, Li M, et al. Gaussian diffusion inpainting for X-ray CT metal artifact reduction. *Biomed Eng Online* 2017;16:1–7.
- [30] Subhas N, Primak AN, Obuchowski NA, et al. Iterative metal artifact reduction: evaluation and optimization of technique. *Skeletal Radiol* 2014;43:1729–35.
- [31] Treece G. Refinement of clinical X-ray computed tomography (CT) scans containing metal implants. *Comput Med Imaging Graph* 2017;56:11–23.
- [32] Subhas N, Polster JM, Obuchowski NA, et al. Imaging of arthroplasties: improved image quality and lesion detection with iterative metal artifact reduction, a new CT metal artifact reduction technique. *AJR Am J Roentgenol* 2016;207:378–85.
- [33] Dobrindt O, Amthauer H, Krueger A, et al. Hybrid SPECT/CT for the assessment of a painful hip after uncemented total hip arthroplasty. *BMC Med Imaging* 2015;2:15–8.
- [34] Messerli M, Rengier F, Desbiolles L, et al. Impact of advanced modeled iterative reconstruction on coronary artery calcium quantification. *Acad Radiol* 2016;23:1506–12.
- [35] Caruso D, De Cecco CN, Schoepf UJ, et al. Correction factors for CT coronary artery calcium scoring using advanced modeled iterative reconstruction instead of filtered back projection. *Acad Radiol* 2016;23:1480–9.
- [36] Schmid AI, Uder M, Lell MM. Reaching for better image quality and lower radiation dose in head and neck CT: advanced modeled and sinogram-affirmed iterative reconstruction in combination with tube voltage adaptation. *Dentomaxillofac Radiol* 2017;46:20160131.